

1           **A total energy error analysis of dynamical cores and**  
2           **physics-dynamics coupling in the Community Atmosphere**  
3           **Model (CAM)**

4           **Peter H. Lauritzen<sup>1\*</sup>, and David L. Williamson<sup>1</sup>**

5           <sup>1</sup>National Center for Atmospheric Research, Boulder, Colorado, USA

6           **Key Points:**

- 7           • Spurious total energy dissipation in dynamical core is  $-0.3W/m^2$  to  $-1W/m^2$  at 1  
8           degree  
9           • Constant-pressure assumption in physics leads to  $0.3W/m^2$  spurious total energy  
10           source  
11           • There can easily be compensating errors in total energy budget

---

\*1850 Table Mesa Drive, Boulder, Colorado, USA

Corresponding author: Peter Hjort Lauritzen, pel@ucar.edu

12 **Abstract**

13 A closed total energy (TE) budget is of utmost importance in coupled climate system  
 14 modeling; in particular, the dynamical core or physics-dynamics coupling should ideally  
 15 not lead to spurious TE sources/sinks. To assess this in a global climate model, a detailed  
 16 analysis of the spurious sources/sinks of TE in NCAR's Community Atmosphere Model  
 17 (CAM) is given. This includes spurious sources/sinks associated with the parameteriza-  
 18 tion suite, the dynamical core, TE definition discrepancies and physics-dynamics coupling.  
 19 The latter leads to a detailed discussion of the pros and cons of various physics-dynamics  
 20 coupling methods commonly used in climate/weather modeling.

21 **1 Introduction**

22 In coupled climate modeling with prognostic atmosphere, ocean, land, land-ice, and  
 23 sea-ice components, it is important to conserve total energy (TE) to a high degree in each  
 24 component individually and in the complete model to avoid spurious long term trends in  
 25 the simulated Earth system. Conservation of TE in this context refers to having a closed  
 26 TE budget. For example, the TE change in a column in the atmosphere is exactly balanced  
 27 by the net sources/sinks given by the fluxes through the column. The fluxes into the at-  
 28 mospheric component from the surface models must be balanced by the fluxes in the re-  
 29 spective surface components and so on. Henceforth we will focus only on the atmospheric  
 30 component which, in a numerical model, is split into a resolved-scale component (the dy-  
 31 namical core) and a sub-grid-scale component (parameterizations or, in modeling jargon,  
 32 physics). While there have been many studies on energy flow in the Earth system through  
 33 analysis of re-analysis data and observations [Trenberth and Fasullo, 2018, and references  
 34 herein], there has been less focus on spurious TE sources/sinks in numerical models.

35 The atmospheric equations of motion conserve TE but the discretizations used in cli-  
 36 mate and weather models are usually not inherently TE conservative. Exact conservation  
 37 is probably not necessary but conservation to within  $\sim 0.01 \text{ W/m}^2$  has been considered  
 38 sufficient to avoid spurious trends in century long simulations [Boville, 2000; Williamson  
 39 *et al.*, 2015]. Spurious sources and sinks of TE can be introduced by the dynamical core,  
 40 physics, physics-dynamics coupling as well as discrepancies between the TE of the con-  
 41 tinuous and discrete equations of motion and for the physics. Hence the study of TE con-  
 42 servation in comprehensive models of the atmosphere quickly becomes a quite complex  
 43 and detailed matter. In addition there can easily be compensating errors in the system as a  
 44 whole.

45 Here we focus on versions of the Community Atmosphere Model (CAM) that use  
 46 the spectral-element [SE, Lauritzen *et al.*, 2018] and finite-volume [FV, Lin, 2004] dy-  
 47 namical cores. These dynamical cores couple with physics in a time-split manner, i.e.  
 48 physics receives a state updated by dynamics [see Williamson, 2002, for a discussion  
 49 of time-split versus process split physics-dynamics coupling in the context of CAM]. In  
 50 its pure time-split form the physics tendencies are added to the state previously produced  
 51 by the dynamical core and the resulting state provides the initial state for the subsequent  
 52 dynamical core calculation. We refer to this as *state-updating* (`ftype=1` in CAM code).  
 53 Alternatively, when the dynamical core adopts a shorter time step than the physics, say  
 54 `nsplit` sub-steps, then  $(1/\text{nsplit})$ th of the physics-calculated tendency is added to the  
 55 state before each dynamics sub-step. We refer to this modification of time-splitting as  
 56 *dribbling* (`ftype=0`). CAM-FV uses the *state-update* (`ftype=1`) approach while CAM-SE  
 57 has options to use *state-update* (`ftype=1`), *dribbling* (`ftype=0`) or a combination of the  
 58 two i.e. mass-variables use *state-updating* and remaining variables use *dribbling*. We refer  
 59 to this as *combination* (`ftype=2`). The *dribbling* variants can lead to spurious sources or  
 60 sinks of TE (and mass) referred to here as physics-dynamics coupling errors.

61 The dynamical core usually has inherent or specified filters to control spurious noise  
 62 near the grid scale which will lead to energy dissipation [Thuburn, 2008; Jablonowski

and Williamson, 2011]. Similarly models often have sponge layers to control the solution near the top of the model that may be a sink of TE. There are examples of numerical discretizations of the adiabatic frictionless equations motion that are designed so that TE is conserved in the absence of time-truncation and filtering errors [e.g., Eldred and Randall, 2017; McRae and Cotter, 2013], e.g., mimetic spectral-element discretizations such as the one used in the horizontal in CAM-SE [Taylor, 2011]. These provide consistency between the discrete momentum and thermodynamic equations leading to global conservation associated with the conversion of potential to kinetic energy. In spectral transform models it is customary to add the energy change due to explicit diffusion on momentum back as heating (referred to as frictional heating), so that the diffusion of momentum does not affect the TE budget [see, e.g., p.71 in Neale et al., 2012]. This is also done in CAM-SE [Lauritzen et al., 2018].

The purpose of this paper is to provide a detailed global TE analysis of CAM. We assess TE errors due to various steps in the model algorithms. The paper is outlined as follows. In section 2 the continuous TE formulas are given and a detailed description of spurious TE sources/sinks that can occur in a model as a whole, and the associated diagnostics used to perform the TE analysis, are defined. In section 3 the model is run in various configurations to assess their effects on TE conservation. This includes various physics-dynamics coupling experiments leading to a rather detailed discussion of mass budget closure. We also investigate the effect of using a limiter in the vertical remapping of momentum, assess energy discrepancy errors and impacts on TE of simplifying surface conditions and dry atmosphere experiments. The paper ends with conclusions.

## 2 Method

### 2.1 Defining total energy (TE)

In the following it is assumed that the model top and bottom are coordinate surfaces and that there is no flux of mass through the model top and bottom. In a dry hydrostatic atmosphere the TE equation integrated over the entire sphere is given by

$$\frac{d}{dt} \int_{z=z_s}^{z=z_{top}} \iint_S E_v \rho^{(d)} dA dz = \int_{z=z_s}^{z=z_{top}} \iint_S F_{net} \rho^{(d)} dA dz, \quad (1)$$

[e.g., Kasahara, 1974] where  $F_{net}$  is net flux calculated by the parameterizations (e.g., heating and momentum forcing),  $d/dt$  the total/material derivative,  $z_s$  is the height of the surface,  $S$  the sphere,  $\rho^{(d)}$  the density of dry air,  $E_v$  is the TE and  $dA$  is an infinitesimal area on the sphere.  $E_v$  can be split into kinetic energy  $K = \frac{1}{2}\mathbf{v}^2$  ( $\mathbf{v}$  is the wind vector), internal energy  $c_v^{(d)}T$ , where  $c_v^{(d)}$  is the heat capacity of dry air at constant volume, and potential energy  $\Phi = gz$

$$E_v = K + c_v^{(d)}T + \Phi. \quad (2)$$

If the vertical integral is performed in a mass-based vertical coordinate, e.g., pressure, then the integrated TE equation for a dry atmosphere can be written as

$$\frac{d}{dt} \int_{p=p_s}^{p=p_{top}} \iint_S E_p dA dp + \frac{d}{dt} \iint_S \Phi_s p_s dA = \int_{p=p_s}^{p=p_{top}} \iint_S F_{net} dA dp, \quad (3)$$

[e.g., Kasahara, 1974] where

$$E_p = K + c_p^{(d)}T. \quad (4)$$

In a moist atmosphere, however, there are several definitions of TE used in the literature related to what heat capacity is used for water vapor and whether or not condensates are accounted for in the energy equation. To explain the details of that we focus on the energy equation for CAM-SE.

CAM-SE is formulated using a terrain-following hybrid-sigma vertical coordinate  $\eta$  but the coordinate levels are defined in terms of dry air mass per unit area ( $M^{(d)}$ ) instead of total air mass;  $\eta^{(d)}$  [see Lauritzen et al., 2018, for details]. In such a coordinate

106 system it is convenient to define the tracer state in terms of a dry mixing ratio instead of  
 107 moist mixing ratio

$$m^{(\ell)} \equiv \frac{\rho^{(\ell)}}{\rho^{(d)}}, \text{ where } \ell = 'wv', 'cl', 'ci', 'rn', 'sw', \quad (5)$$

108 where  $\rho^{(d)}$  is the mass of dry air per unit volume of moist air and  $\rho^{(\ell)}$  is the mass of the  
 109 water substance of type  $\ell$  per unit volume of moist air. Moist air refers to air containing  
 110 dry air ('d'), water vapor ('wv'), cloud liquid ('cl'), cloud ice ('ci'), rain amount ('rn')  
 111 and snow amount ('sw'). For notational purposes define the set of all components of air

$$\mathcal{L}_{all} = \{'d', 'wv', 'cl', 'ci', 'rn', 'sw'\}, \quad (6)$$

112 Define associated heat capacities at constant pressure  $c_p^{(\ell)}$ . We refer to condensates as being  
 113 *thermodynamically and inertially active* if they are included in the thermodynamic  
 114 equation and momentum equations. E.g. if the thermodynamic equation is formulated  
 115 in terms of temperature the energy conversion term includes a generalized heat capacity  
 116 which is a function of the condensates and their associated heat capacities [see, e.g., sec-  
 117 tion 2.3 in *Lauritzen et al., 2018*]. Similarly the weight of the condensates is included in  
 118 the pressure field and pressure gradient force. How many and which condensates are ther-  
 119 modynamically/inertially active in the dynamical core is controlled with namelist `qsize_condensate_loading`.  
 120 If `qsize_condensate_loading=1` only water vapor ('wv') is active, `qsize_condensate_loading=3`  
 121 'wv', 'cl', and 'ci' are active, and if `qsize_condensate_loading=5` then 'wv', 'cl', 'ci', 'rn',  
 122 and 'sw' are included.

123 Using the  $\eta^{(d)}$  vertical coordinate and dry mixing ratios the TE (per unit area) that  
 124 the frictionless adiabatic equations of motion in the CAM-SE dynamical core conserves is

$$\widehat{E}_{dyn} = \frac{1}{\Delta S} \int_{\eta=0}^{\eta=1} \iint_S \left( \frac{1}{g} \frac{\partial M^{(d)}}{\partial \eta^{(d)}} \right) \sum_{\ell \in \mathcal{L}_{all}} \left[ m^{(\ell)} \left( K + c_p^{(\ell)} T + \Phi_s \right) \right] dA d\eta^{(d)}, \quad (7)$$

125 where  $\Delta S$  is the surface area of the sphere,  $\Phi_s$  is the surface geopotential and  $(\cdot)$  refers to  
 126 the global average.

127 In the CAM physical parameterizations a different definition of TE is used. Due to  
 128 the evolutionary nature of the model development, the parameterizations have not yet been  
 129 converted to match the SE dynamical core. For the computation of TE, condensates are  
 130 assumed to be zero and the heat capacity of moisture is the same as for dry air. This is  
 131 equivalent to using a moist mass (dry air plus water vapor) but  $c_p$  of dry air:

$$\widehat{E}_{phys} = \frac{1}{\Delta S} \int_{\eta=0}^{\eta=1} \iint_S \left( \frac{1}{g} \frac{\partial M^{(d)}}{\partial \eta^{(d)}} \right) \left( 1 + m^{(wv)} \right) \left[ \left( K + c_p^{(d)} T + \Phi_s \right) \right] dA d\eta^{(d)}. \quad (8)$$

132 We note that earlier versions of CAM using the spectral transform dynamical core used  
 133  $c_p$  of moist air. The adiabatic, frictionless equations of motion in the CAM-SE dynamical  
 134 core can be made consistent with  $E_{phys}$  by not including condensates in the mass/pressure  
 135 field as well as energy conversion term in the thermodynamic equation and setting the  
 136 heat capacity for moisture to  $c_p^{(d)}$  [Taylor, 2011]. We refer to this version of CAM-SE col-  
 137 orredcombined with *state-updating* (`ftype=1` physics-dynamics coupling as the *energy*  
 138 *consistent* version ; i.e. the same continuous formula for energy is used in both dynamics  
 139 and physics, and there are no physics-dynamics coupling errors.

## 140 2.2 Some remarks on local energy conservation

141 Although this paper focuses on global TE errors, it is important to note that en-  
 142 ergy errors occur locally. For example, whenever an air parcel containing water undergoes  
 143 a phase change (in the parameterizations) its temperature and enthalpy (energy) should  
 144 change but its mass should not. When the air parcel gains or loses water via sedimenta-  
 145 tion or precipitation (or via a fixer or borrower to maintain some physical property like

positive definiteness), then it has implications for the mass and heat content, and heat capacity of the parcel. In turn, that affects the energy and mass of the column and thereby affects the global TE budget. So anything that changes these state variables locally has implications for the TE budget.

An example of an inconsistency in CAM physics is that surface pressure is held fixed during physical parameterization updates but water vapor, and hence surface pressure, does change during sedimentation/precipitation and an inconsistency appears in the mass and energy budget (see item 2 in Section 2.3). Similarly, if a ‘clipper’ is used on water vapor or condensates to avoid (unphysical) negative mixing ratios (more details in section 3.2) and this is not accounted for in the thermodynamics or through a surface flux, that ‘clipping’ will produce an energy source. In the dynamical core TE is not conserved locally in each column as there is a horizontal flux of energy between columns; but the local energy budget should, ideally, be closed and thereby globally TE should be conserved. If a dynamical core does not inherently conserve dry air mass and/or water mass then a spurious source of TE is inevitable (unless fixers are applied).

### 2.3 Spurious energy sources and sinks

In a weather/climate model TE conservation errors can appear in many places throughout the algorithm. Below is a general list of where conservation errors can appear with specific examples from CAM:

1. *Parameterization errors*: Individual parameterizations may not have a closed energy budget ; for example, they may not have been designed to conserve TE or they may conserve a different TE. CAM parameterizations are required to have a closed energy budget under the assumption that pressure remains constant during the computation of the subgrid-scale parameterization tendencies. In other words, the TE change in the column is exactly balanced by the net sources/sinks given by the fluxes through the column.
2. *Pressure work error*: That said, if parameterizations update specific humidity then the surface pressure changes (e.g., moisture entering or leaving the column). In that case the pressure changes which, in turn, changes TE. This is referred to as *pressure work error* [section 3.1.8 in Neale et al., 2012].
3. *Continuous TE formula discrepancy*: If the continuous equations of motion for the dynamical core conserve a TE different from the one used in the parameterizations then an energy inconsistency is present in the system as a whole. This is the case with the new version of CAM-SE that conserves a TE that is more accurate and comprehensive than that used in the CAM physics package as discussed above. As also noted above, this mismatch arose from the evolutionary nature of the model development and not by deliberate design; and should be eliminated in the future.
4. *Dynamical core errors*: Energy conservation errors in the dynamical core, not related to physics-dynamics coupling errors, can arise in multiple parts of the algorithms used to solve the equations of motion. For dynamical cores employing filtering [e.g., limiters in flux operators Lin, 2004] and/or possessing inherent damping which controls small scales, it is hard to isolate their energy dissipation from other errors in the discretization. If a hyperviscosity term or some other diffusion is added to the momentum equation, then one can diagnose the local energy dissipation from such damping and add a corresponding heating to balance it (frictional heating). There may also be energy loss from viscosity applied to other variables such as temperature or pressure which is harder to compensate. Here is a break-down relevant to CAM-SE using a floating Lagrangian vertical coordinate:
  - Horizontal inviscid dynamics: Energy errors resulting from solving the inviscid, adiabatic equations of motion.
  - Hyperviscosity: Filtering errors.

- 197 • Vertical remapping: The vertical remapping algorithm from Lagrangian to Euler-  
 198 ian reference surfaces does not conserve TE.  
 199 • Near round-off negative values of water vapor which are filled to a minimal  
 200 value without compensation.

201 If a dynamical core is not inherently mass-conservative with respect to dry air, wa-  
 202 ter vapor and condensates then TE conservation is affected since

$$\int_{\eta=0}^{\eta=1} \iint_S \left( \frac{1}{g} \frac{\partial M^{(d)}}{\partial \eta^{(d)}} \right) \sum_{\ell \in \mathcal{L}_{all}} [m^{(\ell)}] dA d\eta^{(d)} \quad (9)$$

203 is not conserved. Henceforth we assume that the dynamical core is based on an  
 204 inherently mass-conservative formulation which is the case for CAM-SE and CAM-  
 205 FV.

206 5. *Physics-dynamics coupling (PDC)*: Assume that physics computes a tendency. Usu-  
 207 ally the tendency (forcing) is passed to the dynamical core which is responsible for  
 208 adding the tendencies to the state. PDC energy errors can be split into three types:

- 209 • ‘Dribbling’ errors (or, equivalently, temporal PDC errors): If the TE increment  
 210 from the parameterizations does not match the change in TE when the tenden-  
 211 cies are added to the state in the dynamical core, then there will be a spurious  
 212 PDC error. This will not happen with the *state-update* approach in which the  
 213 tendencies are added immediately after physics and before the dynamical core  
 214 advances the solution in time. The PDC ‘dribbling’ errors can be split into 3 con-  
 215 tributions.:

216 *Thermal energy ‘dribbling’ error*: PDC errors in temperature tendencies occur  
 217 because the  $T$ -increment (call it  $\Delta T$ ) that the parameterizations prescribe leads  
 218 to a dry thermal energy change of  $\Delta M^{(d)} \Delta T$  which will not match the equivalent  
 219 dry thermal energy change when the temperature tendency is added in smaller  
 220 chunks in the dynamical core during the ‘dribbling’ of  $\Delta T$ . The discrepancy  
 221 occurs because  $\Delta M^{(d)}$  changes during each dynamics time-step and hence the  
 222 thermal energy change due to physics forcing accumulated during the ‘dribbling’  
 223 will not equal  $\Delta M^{(d)} \Delta T$ . This error could possibly be eliminated by using ther-  
 224 mal energy forcing instead of temperature increments.

225 *Kinetic energy ‘dribbling’ error*: Similarly, PDC errors in velocity component  
 226 forcing increments ( $\Delta u, \Delta v$ ) occur because the dry kinetic energy change of  $\Delta M^{(d)} [(\Delta u)^2 + (\Delta v)^2]$   
 227 will not match the equivalent dry kinetic energy change when ‘dribbling’ veloc-  
 228 ity component forcing increments ( $\Delta u, \Delta v$ ). It is less clear how to eliminate this  
 229 error as kinetic energy is a quadratic quantity.

230 *Mass ‘clipping’ (affects all TE terms)*: A similar PDC error for mass-variables  
 231 such as vapor vapor forcing, cloud liquid, etc. can occur when the mass-tendencies  
 232 are ‘dribbled’ during the dynamical core integration. The dynamical core trans-  
 233 port of mass variables will move mass around in the horizontal and vertical while  
 234 the ‘dribbled’ physics mass increments are applied in the same location; in that  
 235 situation a negative mass-increment from the parameterizations may be larger  
 236 than the mass available to remove. This can lead to a spurious source mass if  
 237 there is logic in the dynamical core preventing mixing ratios/mass to become  
 238 negative. This is referred to as ‘clipping’ PDC errors and precess is described/discussed  
 239 in detail in Section 3.2.1. The ‘clipping’ change the water mass budget without  
 240 accounting for it in water fluxes or in the thermodynamics and hence lead to a  
 241 TE conservation errors (both kinetic and thermal energy).

- 242 • *Change of vertical grid/coordinate errors*: If the vertical coordinates in physics  
 243 and in the dynamical core are different then there can be spurious PDC energy  
 244 errors even when using the state-update method for adding tendencies to the dy-  
 245 namical core state. For example, many non-hydrostatic dynamical cores [e.g.  
 246 Skamarock et al., 2012] use a terrain-following height coordinate whereas physics  
 247 uses pressure.

- 248 • *Change of horizontal grid errors:* If the physics tendencies are computed on a  
 249 different horizontal grid than the dynamical core then there can be spurious en-  
 250 ergy errors from mapping tendencies and/or variables between horizontal grids  
 251 [e.g., *Herrington et al.*, 2018].
- 252 6. *Compensating Energy fixers:* To avoid TE conservation errors which could accu-  
 253 mulate and ultimately lead to a climate drift, it is customary to apply an arbitrary  
 254 energy fixer to restore TE conservation. Since the spatial distribution of many en-  
 255 ergy errors, in general, is not known, global fixers are used. In CAM a uniform in-  
 256 crement is added to the temperature field to compensate for TE imbalance from all  
 257 processes, i.e. dynamical core, physics-dynamics coupling, TE formula discrepancy,  
 258 energy change due to pressure work **error**, and possibly parameterization errors if  
 259 present.

260 **2.4 Diagnostics**

261 The discrete global averages ( $\widehat{\cdot}$ ) are computed consistent with the discrete model grid  
 262 as outlined in section 2.2. of *Lauritzen et al.* [2014]. The TE global average tendency is  
 263 denoted

$$\partial \widehat{E} \equiv \frac{d\widehat{E}}{dt}. \quad (10)$$

264 By computing the global TE averages  $\widehat{E}$  at appropriate places in the model algorithms,  
 265 we can directly compute  $\partial \widehat{E}$  due to various processes (such as viscosity, vertical remap-  
 266 ping, physics-dynamics coupling, pressure work **error**, etc.) by differencing  $\widehat{E}$  from after  
 267 and before the algorithm takes place. This has been implemented using CAM history in-  
 268 frastructure by computing column integrals of energy at various places in CAM and out-  
 269 putting the 2D energy fields. CAM history internally handles accumulation and averag-  
 270 ing in time at each horizontal grid point. The global averages are computed externally  
 271 from the grid point vertical integrals on the history files (stored in double precision). The  
 272 places in CAM where we compute/capture the grid point vertical integral  $E$  are named us-  
 273 ing three letters where the first letter refers to whether the vertical integral is performed  
 274 in physics ('p') or in the dynamical core ('d'). The trailing two letters refer to the specific  
 275 location in dynamics or physics. For example, 'BP' refers to 'Before Physics' and 'AP'  
 276 to 'After Physics'; the associated total energies are denoted  $E_{pBP}$  and  $E_{pAP}$ , respectively.  
 277 The TE tendency from the parameterizations is the difference between  $E_{pBP}$  and  $E_{pAP}$   
 278 divided by the time-step. The terms and tendencies are then averaged globally externally  
 279 to the model. The pseudo-code in Figure 1 defines the acronyms in terms of where in the  
 280 CAM-SE algorithm the TE vertical integrals are computed and output. For details on the  
 281 CAM-SE algorithm please see *Lauritzen et al.* [2018].

282 Before defining the individual terms in detail we briefly review the model time step-  
 283 ping sequence starting with the physics component as illustrated in Figure 1. The energy  
 284 fixer is applied first to compensate for the spurious net energy change from all compo-  
 285 nents introduced during the previous time step. We will describe this in more detail af-  
 286 ter the various sources and sinks are elucidated. The parameterizations are applied next  
 287 and are required to be energy conserving. They update the state and accumulate the total  
 288 physics tendency (forcing). At this stage the state is saved for use in the energy fixer in  
 289 the next time step. Any changes in the global average energy after this are spurious and  
 290 are compensated by the fixer. The parameterizations update the water vapor but not the  
 291 moist pressure, implying a non-physical change in the dry mass of the atmosphere. The  
 292 dry mass correction corrects the dry mass back to its proper value.

293 The forcing (physics tendency) from the parameterizations is passed to the dynam-  
 294 ical core. If the physics and dynamics operate on different grids, the forcing is remapped  
 295 here. The dynamics operates on a shorter time step **than** the physics and is sub-stepped.  
 296 The remapped **physics increment** is applied to the dynamics state, saved from the end of  
 297 the previous dynamics step, using either *state-updating*, *dribbling*, or *combination* as de-

scribed in the introduction. The dynamics then advances the adiabatic frictionless flow in the floating Lagrangian layers over a further set of sub-steps. Hyperviscosity is applied next with further sub-stepping required for computational stability of the explicit discrete approximations. The energy loss from the specified momentum viscosity is **calculated** locally and is balanced by adding a local change to the temperature, referred to as *frictional heating*. This set of dynamics sub-steps is followed by the vertical remapping from Lagrangian to Eulerian reference layers. The remapping is required to provide layers consistent with the parameterization formulations. The vertical remapping sub-steps are required for stability if the Lagrangian layers become too thin.

At the end of the dynamics, the state is saved to be used by the dynamics the next time step and is also passed to the physics, with a remapping if the dynamics and physics grids differ. At the beginning of the physics the difference in energy between this state and the state saved after the physics during the previous time step is the amount needed to be added or subtracted by the energy fixer. It represents the accumulation of all spurious sources from the dry mass correction, remappings between physics and dynamics grids (if applicable), dynamical core, differing energy definitions (if present), hyerviscosity, and vertical remapping.

We now define the following energy tendencies corresponding to the itemized list in section 2.3 with references to terms indicated in Figure 1. We start just after the energy fixer which will be defined at the end.

1.  $\partial\widehat{E}^{(param)}$ : TE tendency due to parameterizations. In CAM the TE budget for each parameterization is closed (assuming pressure is unchanged) so  $\partial\widehat{E}^{(param)}$  is balanced by net fluxes in/out of the physics columns. Note that this is the only energy tendency that is not spurious since CAM parameterizations have a closed TE budget. This TE tendency is discretely computed as

$$\partial\widehat{E}_{phys}^{(param)} = \frac{\widehat{E}_{pAP} - \widehat{E}_{pBP}}{\Delta t_{phys}}, \quad (11)$$

where  $\Delta t_{phys}$  is the physics time-step (default 1800s) and the subscript *phys* on  $\partial\widehat{E}$  refers to the energy tendency computed in CAM physics.

2.  $\partial\widehat{E}^{(pwork)}$ : Total spurious energy tendency due to pressure work **error**

$$\partial\widehat{E}_{phys}^{(pwork)} = \frac{\widehat{E}_{pAM} - \widehat{E}_{pAP}}{\Delta t_{phys}}. \quad (12)$$

Since CAM-SE dynamical core is based on a dry-mass vertical coordinate the pressure work **error** takes place implicitly in the dynamical core. But the TE tendency due to pressure work **error** is conveniently computed in physics since dynamical cores based on a moist vertical coordinate (e.g., CAM-FV) require pressure and moist mixing ratios to be adjusted for dry mass conservation and tracer mass conservation [section 3.1.8 in *Neale et al.*, 2012]. The difference of TE after and before this adjustment is the TE tendency due to pressure work **error**. In a dry mass vertical coordinate based on dry mixing ratios neither dry mass layer thickness nor dry mixing ratios need to be adjusted to take into account moisture changes in the column. For labeling purposes, the 'total forcing' associated with physics (at least in CAM) consists of parameterizations, pressure work **error** and TE fixer, although strictly speaking the fixer includes components from the dynamics as will be seen.

$$\partial\widehat{E}_{phys}^{(phys)} \equiv \partial\widehat{E}_{phys}^{(param)} + \partial\widehat{E}_{phys}^{(pwork)} + \partial\widehat{E}_{phys}^{(efix)} = \frac{\widehat{E}_{pAM} - \widehat{E}_{pBF}}{\Delta t_{phys}}. \quad (13)$$

where the energy fixer TE tendency is

$$\partial\widehat{E}_{phys}^{(efix)} = \frac{\widehat{E}_{pBP} - \widehat{E}_{pBF}}{\Delta t_{phys}}. \quad (14)$$

- 347 After all the TE budget terms have been defined, the exact composition of  $\partial\widehat{E}_{phys}^{(efix)}$   
 348 will be presented.
- 349 3.  $\partial\widehat{E}^{(discr)}$ : If the physics uses a TE definition different from the TE that the  
 350 continuous equations of motion in the dynamical core conserve (i.e. in the absence of  
 351 discretization errors), then there is a TE discrepancy tendency. This complicates  
 352 the energy analysis as one can not compare TE computed in physics  $\widehat{E}_{phys}$  directly  
 353 with TE computed in the dynamical core  $\widehat{E}_{dyn}$ . This makes errors associated with  
 354 this discrepancy tricky to assess. That said, the TE tendencies computed using the  
 355 dynamical core TE formula  $\partial\widehat{E}_{dyn}$  are well defined (self consistent) and similarly  
 356 for TE tendencies computed using the ‘physics formula’ for TE,  $\partial\widehat{E}_{phys}$ .
- 357 4. The TE tendency from the dynamical core is split into several terms: Horizontal  
 358 adiabatic dynamics (dynamics excluding physics forcing tendency)

$$\partial\widehat{E}_{dyn}^{(2D)} = \frac{\widehat{E}_{dAD} - \widehat{E}_{dBd}}{\Delta t_{dyn}}, \quad (15)$$

359 where over a single dynamics sub-step  $\Delta t_{dyn} = \frac{\Delta t_{phys}}{n_{split} \times r_{split}}$  (the loop bounds  
 360  $n_{split}$ ,  $r_{split}$ , etc. are explained in Figure 1).

361 In CAM-SE the viscosity is explicit so one can compute the TE tendency due to  
 362 hyperviscosity and its associated frictional heating

$$\partial\widehat{E}_{dyn}^{(hvvis)} = \frac{\widehat{E}_{dAH} - \widehat{E}_{dBH}}{\Delta t_{hvvis}}, \quad (16)$$

363 which, in CAM-SE, includes a frictional heating term from viscosity on momentum

$$\partial\widehat{E}_{dyn}^{(fheat)} = \frac{\widehat{E}_{dAH} - \widehat{E}_{dCH}}{\Delta t_{hvvis}}, \quad (17)$$

364 where  $\Delta t_{hvvis} = \frac{\Delta t_{phys}}{n_{split} \times r_{split} \times hypervis\_subcycle}$  is the time step of the sub-stepped  
 365 viscosity. The residual

$$\partial\widehat{E}_{dyn}^{(res)} = \partial\widehat{E}_{dyn}^{(2D)} - \partial\widehat{E}_{dyn}^{(hvvis)}, \quad (18)$$

366 is the energy error due to inviscid dynamics and time-truncation errors.

367 The energy tendency due to vertical remapping is

$$\partial\widehat{E}_{dyn}^{(remap)} = \frac{\widehat{E}_{dAR} - \widehat{E}_{dAD}}{\Delta t_{remap}}, \quad (19)$$

368 where  $\Delta t_{remap} = \frac{\Delta t_{phys}}{n_{split}}$ .

369 The 3D adiabatic dynamical core (no physics forcing but including friction) energy  
 370 tendency is denoted

$$\partial\widehat{E}_{dyn}^{(adiab)} = \partial\widehat{E}_{dyn}^{(2D)} + \partial\widehat{E}_{dyn}^{(remap)}. \quad (20)$$

- 371 5.  $\partial\widehat{E}^{(pdc)}$ : Total spurious energy tendency due to physics-dynamics coupling errors is  
 372 the difference between the energy tendency from physics and the energy tendency  
 373 in the dynamics resulting from adding the physics increment to the dynamical core  
 374 state

$$\partial\widehat{E}^{(pdc)} = \partial\widehat{E}_{phys}^{(phys)} - \partial\widehat{E}_{dyn}^{(phys)} \text{ assuming } \partial\widehat{E}^{(discr)} = 0, \quad (21)$$

375 where

$$\partial\widehat{E}_{dyn}^{(phys)} = \frac{\widehat{E}_{dBd} - \widehat{E}_{dAF}}{\Delta t_{pdc}}, \quad (22)$$

376 and  $\Delta t_{pdc}$  is the time-step between physics increments being added to the dynami-  
 377 cal core. Remember we are dealing with average rates so terms computed with dif-  
 378 ferent time steps can be compared, but differences cannot be taken between terms  
 379 sampled with different time steps.

The physics-dynamics coupling TE tendency  $\partial\widehat{E}^{(pdc)}$  makes use of TE formulas in dynamics and in physics so (21) is only well-defined if the TE formula discrepancy is zero,  $\partial\widehat{E}^{(discr)} = 0$ . As mentioned in Section 2.1, CAM-SE has the option to switch the continuous equations of motion conserving the TE used by CAM physics (8) instead of the more comprehensive TE formula (7).

In CAM-SE there are 3 physics-dynamics coupling algorithms described in detail in section 3.6 in *Lauritzen et al. [2018]* and reviewed in the introduction here. One is *state-update* in which the entire physics increments are added to the dynamics state at the beginning of dynamics (referred to as `ftype=1`), in which case  $\Delta t_{pdc} = \Delta t_{phys}$ . Another is *dribbling* in which the physics tendency is split into `nsplit` equal chunks and added throughout dynamics (more precisely after every vertical remapping; referred to as `ftype=0` resulting in  $\Delta t_{pdc} = \frac{1}{nspit}\Delta t_{phys}$ ), and then a *combination* of the two (referred to as `ftype=2`) where tracers (mass variables) use *state-update* (`ftype=1`) and all other physics tendencies use *dribbling* (`ftype=0`).

6.  $\partial\widehat{E}^{(efix)}$ : Global energy fixer tendency, defined in (14), is applied at the beginning of the parameterizations. The correction needed is the global average difference between the state passed from the dynamics and the state that was saved after the physics updated the state but before the dry mass correction. It includes all spurious sources from the dry mass correction, remappings between physics and dynamics, dynamical core, differing energy definitions (if present), hyperviscosity, and vertical remapping.

## 2.5 A few observations regarding the energy budget terms

It is useful to note that the energy fixer ‘fixes’ energy errors for the dynamical core, pressure work **error**, physics-dynamics coupling and TE discrepancy

$$-\partial\widehat{E}_{phys}^{(efix)} = \partial\widehat{E}_{phys}^{(pwork)} + \partial\widehat{E}_{dyn}^{(adiab)} + \partial\widehat{E}^{(pdc)} + \partial\widehat{E}^{(discr)}. \quad (23)$$

The forcing from the parameterizations,  $\partial\widehat{E}_{phys}^{(param)}$ , does not appear in this budget (although the dynamical core state does ‘feel’ the parameterization forcing) as the energy cycle for the parameterizations is, by design in CAM, closed (balanced by fluxes in/out of the physics columns). If  $\partial\widehat{E}^{(discr)} = 0$ , one can use (23) to diagnose energy dissipation in the dynamical core and physics-dynamics coupling from quantities computed only in physics

$$\partial\widehat{E}_{dyn}^{(adiab)} + \partial\widehat{E}^{(pdc)} = -\partial\widehat{E}_{phys}^{(efix)} - \partial\widehat{E}_{phys}^{(pwork)} \text{ for } \partial\widehat{E}^{(discr)} = 0. \quad (24)$$

This is useful if the diagnostics are not implemented in the dynamical core; in particular, if the *state-update* (`ftype=1`) physics-dynamics coupling method is used then  $\partial\widehat{E}^{(pdc)} = 0$  and the TE errors in the dynamical core can be computed without diagnostics implemented in the dynamical core. Also, (24) provides an alternative formula for  $\partial\widehat{E}^{(pdc)}$  compared to (21):

$$\partial\widehat{E}^{(pdc)} = -\partial\widehat{E}_{phys}^{(efix)} - \partial\widehat{E}_{phys}^{(pwork)} - \partial\widehat{E}_{dyn}^{(adiab)} \text{ assuming } \partial\widehat{E}^{(discr)} = 0. \quad (25)$$

If  $\partial\widehat{E}^{(pdc)} = 0$  (23) can be used to compute  $\partial\widehat{E}^{(discr)}$

$$\partial\widehat{E}^{(discr)} = -\partial\widehat{E}_{phys}^{(efix)} - \partial\widehat{E}_{phys}^{(pwork)} - \partial\widehat{E}_{dyn}^{(adiab)}, \text{ assuming } \partial\widehat{E}^{(pdc)} = 0. \quad (26)$$

Note that we can not use (21) to compute  $\partial\widehat{E}^{(discr)}$  since  $\widehat{E}_{phys} \neq \widehat{E}_{dyn}$ .

## 3 Results

A series of simulations have been performed with CESM2.1 using CAM version 6 (CAM6) physics (<https://doi.org/10.5065/D67H1H0V>) on NCAR’s Cheyenne cluster [*Computational and Information Systems Laboratory, 2017*]. All simulations are at nominally  $\sim 1^\circ$  horizontal resolution (for CAM-SE that is 30×30 elements on each cubed-sphere face and for CAM-FV its 192×288 latitudes-longitudes) and using the standard

**Table 1.** TE tendencies in units of  $W/m^2$  associated with various aspects of CAM-SE run in AMIP-type setup (unless otherwise noted). Column 1 is the identifier for the model configuration. See the text for a brief summary of these descriptors. They are defined in more detail in the following sections where the section titles also include the ‘Descriptor’ from Table 1 to make it easier for the reader to match Table entries with discussion in the text. Column 2 is  $\mathcal{N}$  =qsize\_condensate\_loading identifying how many water species are thermodynamically/inertially active in the dynamical core (see section 2.1 for details). Column 3, lcp\_moist, indicates whether or not the heat capacity includes water variables or not and column 4 shows physics-dynamics coupling method ftype. The TE tendencies  $\partial \widehat{E}$  in columns 5-14 are defined in section 2.4. If  $\partial \widehat{E}$  is less than  $10^{-5} W/m^2$  it is set to zero in the Table. Significant changes compared to the baseline (TE consistent configuration) discussed in the main text are in bold font. Entries marked with ‘-’ refer to TE tendencies that can not be directly calculated with the current framework.

Descriptor	$\mathcal{N}$	lcp_moist	ftype	$\partial \widehat{E}_{phys}^{(pwork)}$	$\partial \widehat{E}_{phys}^{(fix)}$	$\partial \widehat{E}_{phys}^{(discr)}$	$\partial \widehat{E}_{dyn}^{(2D)}$	$\partial \widehat{E}_{dyn}^{(heat)}$	$\partial \widehat{E}_{dyn}^{(res)}$	$\partial \widehat{E}_{dyn}^{(remap)}$	$\partial \widehat{E}_{dyn}^{(adiab)}$	$\partial \widehat{E}^{(pdc)}$
<i>TE consistent</i>	1	false	1	0.312	0.300	0	-0.601	-0.608	0.565	0.007	-0.011	-0.613
‘dribbling’ A	1	false	0	0.315	0.313	0	-0.577	-0.584	0.568	0.007	-0.011	-0.588
‘dribbling’ B	1	false	2	0.316	0.341	0	-0.598	-0.606	0.563	0.008	-0.011	-0.609
vert limiter	1	false	1	0.317	0.472	0	-0.590	-0.597	0.509	0.006	<b>-0.199</b>	-0.789
smooth topo	1	false	1	0.315	<b>-0.008</b>	0	<b>-0.295</b>	<b>-0.300</b>	0.493	0.005	-0.012	<b>-0.307</b>
energy discr	5	true	1	0.332	-0.313	<b>0.594</b>	-0.603	-0.612	0.575	0.009	-0.011	-0.614
default	5	true	2	0.316	-0.272	-	-0.578	-0.587	0.579	0.010	-0.012	-0.589
<i>QPC6</i>	1	false	1	0.305	-0.169	0	<b>-0.129</b>	<b>-0.131</b>	0.477	0.001	-0.007	<b>-0.136</b>
<i>FHS94</i>	1	false	2	-	-	-	<b>-0.025</b>	<b>-0.025</b>	0.122	0	0.005	<b>-0.020</b>
<i>FV</i>	1	false	1	0.304	0.670	0	-	-	-	-	-	<b>-0.974</b>
<i>CSLAM</i>	1	false	1	0.312	0.239	0	-0.547	-0.557	0.620	0.010	-0.011	-0.558
<i>CSLAM default</i>	5	true	2	0.320	-0.342	-	-0.524	-0.537	0.641	0.013	-0.011	-0.535

423 32 levels in the vertical. Unless otherwise noted all simulations are 13 months in dura-  
 424 tion and the last 12 months are used in the analysis. Total energy budgets are summarized  
 425 in Table 1 and discussed below. The first column gives identifying ‘Descriptors’ which  
 426 are briefly summarized below and defined in more detail in the following sections. The  
 427 section titles also include the ‘Descriptor’ from Table 1 to make it easier for the reader  
 428 to match Table entries with discussion in the text. Important changes to TE errors are  
 429 marked with bold font in Table 1.

430 Various configurations are used and referred to in terms of the *COMPSET* (Com-  
 431 ponent Set) value used in CESM2.1 The *COMPSET F2000climo* configuration refers  
 432 to ‘real-world’ AMIP (Atmospheric Model Intercomparison Project) type simulations us-  
 433 ing perpetual year 2000 SST (Sea Surface Temperature) boundary conditions. The first 7  
 434 simulations in the table (those above the horizontal line) are such AMIP-type simulations  
 435 (*F2000climo*) with the first serving as a control for the 6 following variants. The remain-  
 436 ing 5 simulation descriptors (below the horizontal line in Table 1) list their *COMPSET* or  
 437 dynamical core settings.

- 438 • *TE consistent*: The TE consistent version uses *state update* physics-dynamics cou-  
 439 pling (*ftype* 1) described in section 3.1,
- 440 • ‘*dribbling*’ A: as *TE consistent* but with *dribbling* physics-dynamics coupling (*ftype*  
 441 0) (section 3.2),
- 442 • ‘*dribbling*’ B: as *TE consistent* but with *dribbling* combination physics-dynamics  
 443 coupling (*ftype* 2) (section 3.2),
- 444 • *vert limiter*: as *TE consistent* but using limiters in the vertical remapping of mo-  
 445 mentum (section 3.3),
- 446 • *smooth topo*: as *TE consistent* but using smoother topography (see section 3.4),
- 447 • *energy discr*: The version with energy discrepancy (but no physics-dynamics cou-  
 448 pling errors) described in section 3.5,
- 449 • *default*: as *energy discr* version but with *ftype*=2 which is the current default  
 450 CAM-SE (section 3.5),
- 451 • *QPC6*: A simplified aqua-planet setup based on the *TE consistent*, i.e an aqua-  
 452 planet setup using CAM6 physics; an ocean covered planet in perpetual equinox,  
 453 with fixed, zonally symmetric sea surface temperatures [Neale and Hoskins, 2000;  
 454 Medeiros et al., 2016] (section 3.6),
- 455 • *FSH94*: Dry dynamical core configuration based on Held-Suarez forcing which re-  
 456 laxes temperature to a zonally symmetric equilibrium temperature profile and sim-  
 457 ple linear drag at the lower boundary [Held and Suarez, 1994] (section 3.7),
- 458 • *FV*: A configuration with the SE dynamical core replaced with the finite-volume  
 459 core (section 3.8), and
- 460 • *CSLAM*: The quasi equal-area physics grid configuration of CAM-SE based on the  
 461 TE consistent setup (section 3.9)
- 462 • *CSLAM default*: Same as *CSLAM* configuration but with *ftype*=2 and all forms of  
 463 water thermodynamically/*inertially* active in the dynamical core.

### 470 3.1 *TE consistent: state-update* physics-dynamics coupling (*ftype*=1) and no TE 471 formula discrepancy

472 This configuration is the most energetically consistent in that the physical parame-  
 473 terizations and the continuous equations of motion on which the dynamical core is based,  
 474 conserve the same TE (defined in equation (8)); and there are no spurious sources/sinks in  
 475 physics-dynamics coupling. Energetic consistency in dynamics and physics is obtained  
 476 by setting  $c_p^{(\ell)} \equiv c_p^d$  and  $\mathcal{L}_{all} = \{\text{`d', 'wv'}\}$  in the dynamical core equations of mo-  
 477 tion and TE computations. Associated namelist changes resulting in this configuration are  
 478 `lcp_moist = .false., se_qsize_condensate_loading = 1, and ftype = 1.`

The TE consistent configuration in AMIP-type simulation (*F2000climo*) is used to compute baseline TE tendencies which will be used to compare with other model configurations. First we establish how long an average is needed to get robust TE tendency estimates. Figure 2 shows  $\partial\widehat{E}$  for various aspects of CAM-SE as a function of time. The simulation length is 5 years and monthly average values are used for the analysis. First consider the left plot. The TE tendency from parameterizations ( $\partial\widehat{E}_{phys}^{(param)}$ ) show significant variability with an amplitude of approximately  $2.5W/m^2$ . As noted above this term does not figure in the spurious TE budget. The net source/sink provides an equal and opposite term to balance it. That said, the variability is reflected onto the TE tendency due to pressure work **error**  $\partial\widehat{E}_{phys}^{(pwork)} \approx 0.32 \pm 0.08W/m^2$ . On the scale used in the left-hand plot the TE tendency of the adiabatic dynamical core  $\partial\widehat{E}_{dyn}^{(adiab)}$  does not seem to be affected by  $\partial\widehat{E}_{phys}^{(param)}$  or  $\partial\widehat{E}_{phys}^{(pwork)}$  in terms of variability, and remains stable at approximately  $-0.6W/m^2 \pm 0.02W/m^2$ . The TE fixer, in this model configuration, fixes  $\partial\widehat{E}_{dyn}^{(adiab)}$  and  $\partial\widehat{E}_{phys}^{(pwork)}$ . Since the TE imbalance in the adiabatic dynamics remains approximately constant and the TE tendency associated with pressure work **error** has variability, the TE tendency from the  $\partial\widehat{E}_{phys}^{(efix)}$  has variability;  $\partial\widehat{E}_{phys}^{(efix)} \approx 0.30 \pm 0.08W/m^2$ . As a consistency check  $-\partial\widehat{E}_{dyn}^{(adiab)} - \partial\widehat{E}_{phys}^{(pwork)}$  is plotted with asterisk's and they coincide (as expected) with  $\partial\widehat{E}_{phys}^{(efix)}$  fulfilling (23).

The right-hand plot in Figure 2 shows a breakdown of the dynamical core TE tendencies. The majority of the TE errors are due to hyperviscosity on temperature and pressure,  $\partial\widehat{E}_{dyn}^{(hvis)} \approx -0.61 \pm 0.01W/m^2$ . The diffusion of momentum is added back as frictional heating and is therefore not part of  $\partial\widehat{E}_{dyn}^{(hvis)}$ . The frictional heating is a significant term in the TE tendency budget  $\partial\widehat{E}_{dyn}^{(fheat)} \approx 0.56 \pm 0.02W/m^2$  and exhibits some variability but with a rather small amplitude. The remaining TE error in the floating Lagrangian dynamics is inviscid dissipation and time-truncation errors  $\partial\widehat{E}_{dyn}^{(res)} = \partial\widehat{E}_{dyn}^{(2D)} - \partial\widehat{E}_{dyn}^{(hvis)} \approx 0.007W/m^2$ . The TE tendency from vertical remapping is approximately  $\partial\widehat{E}_{dyn}^{(remap)} \approx -0.01W/m^2$ . To within  $\sim 0.02W/m^2$  the dynamical core TE tendency terms can be computed from just one month average TE integrals. The TE tendencies computed in physics, excluding  $\partial\widehat{E}_{phys}^{(param)}$ , exhibit more variability and are only accurate to  $\sim 0.1W/m^2$  after a one month average.

While it is advantageous to use *state-update* physics-dynamics coupling algorithm (`fptype=1`) in terms of having no spurious TE tendency from coupling,  $\partial\widehat{E}^{(pdc)} = 0$ , it does result in spurious gravity waves in the simulations [see, e.g., Figure 5 in *Gross et al., 2018*]. Figure 3a shows a 1 year average of  $|\frac{dp_s}{dt}|$ , a measure of high frequency gravity wave noise. It clearly exhibits unphysical oscillations coinciding with element boundaries. Details of the spectral-element method, its coupling to physics and associated noise issues are discussed in detail in *Herrington et al. [2018]*. The noise in the solutions is even visible in the 500hPa pressure velocity annual average (Figure 4a). This issue can be alleviated by using a shorter physics time-step so that the physics increments are smaller (not shown). Climate modelers have historically not pursued a shorter physics time-step in production configurations as climate parameterizations are computationally expensive and there is a large sensitivity to physics time-steps in the simulated climate [e.g. *Williamson and Olson, 2003; Wan et al., 2015*].

### 524 3.2 ‘dribbling’ A/B: Non-TE conservative physics-dynamics coupling (`fptype=0, 2`)

525 Before discussing the impact of different PDC methods on the TE budget, we discuss  
526 element boundary noise issues in CAM-SE which are related to PDC method. This  
527 motivates the different PDC methods implemented in CAM-SE.

528            **3.2.1 Spurious element boundary noise from physics-dynamics coupling**

529       When switching to *dribbling* physics-dynamics coupling algorithm (`ftype=0`) in  
 530       which the tendencies from physics are added throughout the dynamics (in this case twice  
 531       per physics time-step) then the noise issues described in previous section disappear (Figure  
 532       3b and 4b). That said, there is a significant issue with this approach; the tracer mass bud-  
 533       get may not be closed. How this comes about is illustrated in Figure 5 and explained in  
 534       the next paragraph.

535       The orange curve on Figure 5a, b, d, and e is the initial state of, e.g., cloud liq-  
 536       uid mixing ratio as a function of location, e.g., longitude. Cloud liquid is zero outside  
 537       of clouds and hence provides a good example for the purpose of this illustration. The  
 538       light blue arrows show the increments (in terms of length of arrow) computed by the pa-  
 539       rameterizations based on the initial state and scaled for the partial update with *dribbling*  
 540       (`ftype=0`). With *state-update* (`ftype=1`) the increments from physics are added to the  
 541       dynamical core state (dotted line on 5b) before the dynamical core advances the solution  
 542       in time. The parameterizations are designed to not drive the mixing ratios negative so the  
 543       state-update in dynamics will not generate negatives (or overshoots). Then the dynami-  
 544       cal core advects the distribution (solid curve on Figure 5c). With *dribbling* (`ftype=0`) the  
 545       physics increments are split into equal chunks (in this illustration two; blue errors on Fig-  
 546       ure 5d). Half of the physics increments are added to the initial state (dotted line on Fig-  
 547       ure 5e) and then dynamics advects the distribution half of the total dynamical core steps  
 548       (dashed line on Figure 5e). Then the other half of the physics increments are applied (in  
 549       the same location as they were computed by physics). Now after the previous/first advec-  
 550       tion step the cloud liquid distribution has moved and the mixing ratio may be zero (or  
 551       less than the increment prescribed by physics) where the physics forcing is applied (e.g.,  
 552       left side of dashed curve). Hence the physics increment is driving the mixing ratios neg-  
 553       ative in those locations. Thereafter the distribution is advected (solid curve on Figure 5f).  
 554       In CAM the increments added in the dynamical core are limited so that they drive the  
 555       mixing to zero (but not negative) if this problem occurs. This leads to a net source of  
 556       mass compared to the mass change that the parameterizations prescribe (see Figure 6).  
 557       Although the average source of mass is small each time-step it always has the same sign  
 558       (i.e. it is a bias) and therefore accumulates. Zhang *et al.* [2017] estimated that this spuri-  
 559       ous source of mass is equivalent to  $\sim 10\text{cm}$  sea-level rise per decade in coupled climate  
 560       simulation experiments.

561       The majority of the noise with *state-update* (`ftype=1`) physics-dynamics coupling  
 562       method comes from momentum sources/sinks and heating/cooling. A way to alleviate  
 563       noise problems and, at the same time, close the tracer mass budgets (in physics-dynamics  
 564       coupling) is to use *state-update* (`ftype=1`) coupling for tracers and *dribbling* (`ftype=0`)  
 565       coupling for momentum and temperature (referred to as *combination*, `ftype=2`). Figure  
 566       3c shows the noise diagnostic  $|\frac{dp_s}{dt}|$  for *combination* (`ftype=2`) coupling. Figure 3c looks  
 567       very similar to Figure 3b but there is some noise near element boundaries. That said, in  
 568       terms of vertical pressure velocities *combination* (`ftype=2`) and *dribbling* (`ftype=0`) cli-  
 569       mates are similar in terms of the level of noise (Figure 4b and 4c). The element noise in  
 570       CAM-SE with *combination* (`ftype=2`) seen in both  $|\frac{dp_s}{dt}|$  and 500hPa pressure velocity  
 571       can be ‘removed’ by using CAM-SE-CSLAM (Figure 3d) which uses a quasi equal-area  
 572       physics grid and CSLAM [Conservative Semi-LAgrangian Multi-tracer; Lauritzen *et al.*,  
 573       2010] consistently coupled to the SE method [Lauritzen *et al.*, 2017]. The noise patterns  
 574       in vertical velocity off the western coast of South America are present in all CAM-SE  
 575       simulations (and hence not related to physics-dynamics coupling algorithm) are also ‘re-  
 576       moved’ by using CAM-SE-CSLAM [Herrington *et al.*, 2018].

577            **3.2.2 Spurious TE tendencies from physics-dynamics coupling**

578       When using the same TE formula in the dynamical core and physics the spurious  
 579       TE tendency from physics-dynamics coupling can be assessed. As described in item 5  
 580       ([Section 2.3](#)), PDC errors can be attributed to underlying pressure changes during the  
 581       ‘dribbling’ of temperature and velocity component increments as well as PDC ‘clipping’  
 582       errors in the water variables (the process in which ‘clipping’ occurs is described in detail  
 583       in the previous subsection). The TE error associated with ‘clipping’ PDC error occurs due  
 584       to the mass-change prescribed by physics consistent with the fluxes in/out of the physics  
 585       column does not equal the actual mass change applied to the dynamical core state due to  
 586       ‘clipping’

587       For `ftype=2` PDC only the increment for temperature and momentum are *dribbled*  
 588       whereas tracer mass is state-updated (no ‘clipping’ errors). This results in a spurious PDC  
 589       TE tendency of  $\partial\widehat{E}^{(pdc)} = -0.484W/m^2$ . When using `ftype=0` PDC also tracer increments  
 590       are *dribbled* (hence there are ‘clipping’ PDC errors) a similar TE tendency results  
 591        $\partial\widehat{E}^{(pdc)} = -0.469W/m^2$ . The difference between the TE PDC tenendency for `ftype=2`  
 592       and `ftype=0` provides an estimate of the TE PDC ‘clipping’ error. The ‘clipping’ PDC  
 593       TE tenendency is very small  $0.015W/m^2$ .

594            **3.3 vert limiter: Limiters on vertical remapping of momentum**

595       CAM-SE uses a floating Lagrangian vertical coordinate [[Starr, 1945](#); [Lin, 2004](#)]  
 596       which requires the remapping of the atmospheric state from floating levels back to refer-  
 597       ence levels to maintain computational stability and to provide state data consistent with  
 598       the physics formulation. The mapping algorithm is based on the mass conservative PPM  
 599       (Piecewise Parabolic Method) with options for shape-preserving limiters. In CAM-SE mo-  
 600       mentum components and internal energy are used as the variables mapped in the vertical  
 601       [[Lauritzen et al., 2018](#)] and, contrary to earlier versions of CAM-SE, there is no limiter  
 602       on the remapping of wind components. If the shape-preserving limiter is used for mo-  
 603       mentum mapping then the TE dissipation increases by over an order of magnitude from  
 604        $\sim 0.01W/m^2$  to  $\sim 0.2W/m^2$  (Table 1).

605            **3.4 smooth topo: Smoother topography**

606       Topography for CAM is generated using a new version of the software/algorithm de-  
 607       scribed in [Lauritzen et al. \[2015\]](#) that is available at <https://github.com/NCAR/Topo>.  
 608       The updates to the software includes smoothing algorithms and the computation of sub-  
 609       grid-scale orientation of topography.

610       The default topography in CAM-SE uses the same amount of topography smooth-  
 611       ing as CAM-FV (distance weighted smoother applied to the raw topography on  $\sim 3\text{km}$   
 612       cubed-sphere grid with a smoothing radius of 180km referred to as C60). When the to-  
 613       polography is smoother (in this case using C92 smoothing, i.e. smoothing radius of approx-  
 614       imately 276km) the hyperviscosity operators are less active leading to reduced TE errors,  
 615       i.e.  $\partial\widehat{E}_{dyn}^{(hv)}$  is reduced in half from approximately  $-0.6W/m^2$  to  $-0.3W/m^2$ . The vertical  
 616       remapping TE error, however, remains approximately the same. Since the pressure work  
 617       [error](#) is approximately  $0.3W/m^2$  it almost exactly compensates for the TE tendency from  
 618       the dynamical core  $\partial\widehat{E}_{dyn}^{(adiab)}$ . Hence if one would only diagnose the TE tendency from  
 619       the energy fixer one could mistakenly conclude that the model universally conserves TE  
 620       when, in fact, there are compensating TE errors in the system. These compensating errors  
 621       can only be diagnosed through a careful breakdown of the total TE tendencies.

### 622 3.5 default: TE formula discrepancy errors

623 To assess the TE errors due to the discrepancy in the energy formula used by dy-  
 624 namics and physics, a simulation using *state-updating* (*f<sub>type</sub>*=1, no ‘*dribbling* errors) and  
 625 thermodynamically/*inertially* active condensates in the dynamical core (*qsize\_condensate\_loading* =  
 626 5) and consistent/accurate associated heat capacities  $c_p^{(\ell)}$  (namelist *lcp\_moist=.true.*)  
 627 has been performed. In this setup the continuous equations of motion in the dynami-  
 628 cal core conserve an energy different from physics, and the energy fixer will restore the  
 629 ‘physics’ version of energy. Despite the dynamical core now using a more comprehensive  
 630 formula for energy, the TE dissipation terms in the dynamical core are roughly the same  
 631 as in the energy consistent versions of the model. Using (26) we can assess the TE energy  
 632 discrepancy errors which result in  $\sim 0.59W/m^2$ . *Taylor* [2011] found a similar result just  
 633 from using the more comprehensive formula for heat capacity (based on dry air and water  
 634 vapor) and not including thermodynamically/*inertially* active condensates. As noted before  
 635 this formulation inconsistency is due to the evolutionary nature of CAM development and  
 636 it is the intention to remove this inconsistency in future versions of the model.

637 The default version of CAM-SE uses this configuration but with *combination* (*f<sub>type</sub>*=2)  
 638 which has similar TE characteristics (see Table 1). That said, the physics-dynamics cou-  
 639 pling error from *dribbling* momentum and temperature tendencies and the energy discrep-  
 640ancy errors can not be separated in this configuration:

$$\partial\widehat{E}^{(pdc)} + \partial\widehat{E}^{(discr)} = 0.546W/m^2, \quad (27)$$

641 using (23). With *state-updating* (*f<sub>type</sub>*=1) (i.e.  $\partial\widehat{E}^{(pdc)} = 0$ ) the energy discrepancy error  
 642 was  $0.594W/m^2$  and in the energy consistent setup (i.e.  $\partial\widehat{E}^{(discr)} = 0$ ) but using *dribbling*  
 643 (*f<sub>type</sub>*=2) we got  $\partial\widehat{E}^{(pdc)} = 0.484W/m^2$ . So if the physics-dynamics coupling errors  
 644 and energy discrepancy errors in the different configurations would be additive, one would  
 645 have expected  $\partial\widehat{E}^{(pdc)} + \partial\widehat{E}^{(discr)}$  to be over  $1W/m^2$  which is clearly not the case (27).  
 646 Again, it must be concluded that there are canceling errors in the system.

#### 647 3.5.1 2D structure of TE errors

653 Figure 7 shows the two-dimensional spatial structure of column-integrated TE ten-  
 654 dencies for the *default* configuration. The first plot (Figure 7a) shows column inte-  
 655 grated  $\partial E^{(param)}$ , i.e. the spatial structure of ‘physical’ TE tendency. Only contours from  
 656  $\pm 150W/m^2$  are shown although the actual range (noted above color bar) is  $-148.3W/m^2$  to  
 657  $1770W/m^2$ . The larger positive values are only for a small number of grid points (moun-  
 658 tains of New Guinea). The column-integrated dynamical core TE tendency  $\partial\widehat{E}^{(adiab)}$   
 659 (Figure 7c) approximately balances  $\partial E^{(param)}$ . The TE pressure work error tendency  
 660  $\partial E^{(pwork)}$  (Figure 7b) is, as expected, largest where precipitation and evaporation is largest.  
 661 The last 3 plots show terms in the dynamical core budget: column-integrated TE ten-  
 662 dency for hyperviscosity,  $\partial\widehat{E}^{(hvvis)}$ , vertical remapping,  $\partial\widehat{E}^{(remap)}$ , and frictional heating,  
 663  $\partial\widehat{E}^{(fheat)}$ . Compared to  $\partial E^{(param)}$  the hyperviscosity tendencies  $\partial\widehat{E}^{(hvvis)}$  are very large  
 664 meaning that the frictionless adiabatic dynamical core creates very large TE tendencies  
 665 (not shown) that are, to a large degree, compensated for by the hyperviscosity operators.  
 666 Otherwise the total dynamical core TE tendencies would be equally large. The frictional  
 667 heating TE tendency is largest over/near topography. Similarly for vertical remapping but,  
 668 in addition, there are large TE tendencies in areas of large updrafts/downdrafts over ocean.

### 670 3.6 QPC6: Simplified surface

671 By running the model in aqua-planet configuration one can assess the effect of sim-  
 672 plifying the surface boundary condition. In particular, without topography forcing the dy-  
 673 namical core is not challenged with respect to stationary near-grid-scale forcing. The TE  
 674 tendency with respect to pressure work *error* remains the same  $\partial\widehat{E}_{phys}^{(pwork)}$  as the AMIP-

675 type simulations, however, the adiabatic dynamical core TE tendency reduces to  $\partial\widehat{E}_{dyn}^{(adiab)} =$   
 676  $-0.14W/m^2$  (approximately a factor 4 reduction). Most of that reduction is due to viscosity  
 677  $\partial\widehat{E}_{dyn}^{(hvis)} = -0.13W/m^2$ . The frictional heating is roughly the same as AMIP  $\partial\widehat{E}_{dyn}^{(fheat)} =$   
 678  $0.48W/m^2$  as is the vertical remapping  $\partial\widehat{E}_{dyn}^{(remap)} = -0.01W/m^2$ . To evaluate the dynam-  
 679 ical cores diffusion of TE it is therefore important to asses the model in a configuration  
 680 with topography as the wave dynamics generated by topography leads to more active dif-  
 681 fusion operators.

### 682 3.7 FHS94: Simplified physics (no moisture)

683 Simplifying the setup even further by replacing the parameterizations with relax-  
 684 ation towards a zonally symmetric temperature profile and simple boundary layer friction  
 685 (Held-Suarez forcing) as well as excluding moisture, the TE errors in the dynamical core  
 686 decreases even further to  $\sim 0.002W/m^2$  since there is no small scale forcing. Small scales  
 687 are only created by the nonlinear dynamics and the physics works to damp them. Hyper-  
 688 viscosity is less active leading to significant reductions compared to aqua-planet and ‘real-  
 689 world’ simulation results. The TE diffusion in vertical remapping reduces by an order of  
 690 magnitude compared to the aqua-planet simulations ( $\sim 0.0005W/m^2$ ). This further em-  
 691 phasizes that TE diffusion assessment in a simplified setup is not necessarily telling for  
 692 the dynamical cores performance with moist physics and topography that challenge the  
 693 dynamical core in terms of strong grid-scale forcing.

### 694 3.8 FV: Changing dynamical core to Finite-Volume (FV)

695 As a comparison the TE error characteristics of the CAM-FV dynamical core are  
 696 assessed. Although the TE diagnostics have not been implemented in the CAM-FV dy-  
 697 namical core, the TE diagnostics in CAM physics are independent of dynamical core  
 698 and can therefore be activated with CAM-FV. The CAM-FV dynamical core uses *state-*  
 699 *update* physics-dynamics coupling (`fptype=1`) ( $\partial\widehat{E}^{(pdc)} = 0$ ) and the same TE definition  
 700 as CAM physics ( $\partial\widehat{E}^{(discr)} = 0$ ). Hence (24) can be used to compute the TE errors of  
 701 the CAM-FV dynamical core,  $\partial\widehat{E}_{dyn}^{(adiab)} \approx -1W/m^2$ . As we do not have the **breakdown**  
 702 of  $\partial\widehat{E}_{dyn}^{(adiab)}$  it can not be determined how much of the TE errors are due to the vertical  
 703 remapping. Furthermore, CAM-FV contains intrinsic dissipation operators (limiters in the  
 704 flux operators) making it difficult to assess TE sources/sinks due to dissipation. Note that  
 705 the pressure work **error** even with a change of dynamical core remains approximately the  
 706 same as the CAM-SE configurations.

### 707 3.9 CSLAM: Quasi equal-area physics grid

708 This configuration was discussed in the context of element noise in section 3.2.1.  
 709 By averaging the dynamics state of an equal-partitioning (in central angle cubed-sphere  
 710 coordinates) of the elements, the element-boundary noise found in CAM-SE can be re-  
 711 moved. Lauritzen *et al.* [2018] argue that this way of computing the state for the physics  
 712 is more consistent with physics in terms of providing a cell-averaged state instead of ir-  
 713 regularly spaced point (quadrature) values. In order to achieve a closed mass-budget, this  
 714 configuration uses CSLAM for tracer transport rather than SE transport. That said, the  
 715 physics columns no longer coincide with the quadrature grid and there are TE errors asso-  
 716 ciated with mapping state and tendencies between the two grids.

717 In this configuration the energy diagnostics computed in the dynamical core are  
 718 computed on the quadrature grid and the energy diagnostics computed in physics are on  
 719 the physics grid. If the TE consistent configuration is used (`fptype=1, qsize_condensate_loading=1,`  
 720 `lcp_moist=.false.`) then the physics-dynamical coupling errors,  $\widehat{E}^{(pdc)}$  computed with  
 721 (21), are entirely due to mapping state from quadrature grid to physics grid and map-

722 ping tendencies back the quadrature grid from the physics grid. The results is  $\widehat{E}^{(pdc)} =$   
 723  $-0.07W/m^2$  which is a rather small error compared to other terms in the TE budget.

724 Due to similar noise problems with CAM-SE-CSLAM when using ftype=1 that  
 725 were observed in CAM-SE (Figure 3 and 4), the default version of CAM-SE-CSLAM uses  
 726 ftype=2. Again physics-dynamics coupling errors and TE discrepancy errors can not be  
 727 separated;  $\partial\widehat{E}^{(pdc)} + \partial\widehat{E}^{(discr)} = 0.557W/m^2$ .

## 728 4 Conclusions

729 A detailed total energy (TE) error analysis of the Community Atmosphere Model  
 730 (CAM) using version 6 physics (included in the CESM2.1 release) running at approxi-  
 731 mately  $1^\circ$  horizontal resolution has been presented. In the global climate model there can  
 732 be many spurious contributions to the TE budget. These errors can be divided into four  
 733 categories: physical parameterizations, adiabatic dynamical core, the coupling between  
 734 physics and dynamics, and TE definition discrepancies between dynamics and physics.  
 735 The latter is not by design but through the evolutionary nature of model development. By  
 736 capturing the atmospheric state at various locations in the model algorithm, a detailed  
 737 budget of TE errors can be constructed. The net spurious TE energy errors are com-  
 738 pensated with a global energy fixer (providing a global uniform temperature increment) every  
 739 physics time-step.

740 In CAM physics the parameterizations have, by design, a closed energy budget (change  
 741 in TE is balanced by fluxes in/out the top and bottom of physics columns) if it is assumed  
 742 that pressure is not modified. However, the pressure changes due to fluxes of mass (e.g.,  
 743 water vapor) in/out of the column which changes energy (referred to as pressure work  
 744 **error**). The pressure work **error** with the full moist physics configuration is very stable  
 745 across different configurations at  $\sim 0.3W/m^2$ . The TE errors in the spectral element (SE)  
 746 dynamical core varies across configurations. Aspects that influence TE is the presence  
 747 of topography, the amount of topography smoothing and moist physics. By smoothing  
 748 topography more the TE error is cut in half from  $\sim -0.6W/m^2$  to  $\sim -0.3W/m^2$ ; and re-  
 749 duces by a factor of **six** ( $\sim -0.1W/m^2$ ) if no topography is present at all (aqua-planet  
 750 configuration). Moist physics forcing also contributes significantly to the TE budget. For  
 751 example, in the dry Held-Suarez setup TE dissipation of the SE dynamical core reduces  
 752 to  $-0.03W/m^2$ . Topography and moist physics force the dynamical core at the grid scale  
 753 and hence the viscosity operators are more active. Consistent with this statement is that  
 754 the changes in TE discussed so far are almost entirely due to the viscosity operator TE  
 755 dissipation. For CAM-SE the spurious TE dissipation in the adiabatic dynamical core is  
 756  $\sim -0.6W/m^2$  in ‘real-world’ configurations. For comparison, CAM-FV’s spurious TE  
 757 change due to the adiabatic dynamical core is  $\sim -1W/m^2$ .

758 By further breaking down the TE dissipation in the SE dynamical core it is ob-  
 759 served the vertical remapping accounts for only  $\sim -0.01W/m^2$ . That said, if the shape-  
 760 preserving limiters in the vertical remapping are invoked the TE dissipation increases 20-  
 761 fold to  $\sim -0.2W/m^2$ . In CAM-SE the kinetic energy dissipation is added as heating in  
 762 the thermodynamic equation (also referred to as frictional heating). The frictional heat-  
 763 ing remains very stable across configurations that include moisture ( $\sim 0.5W/m^2$ ) and re-  
 764 duces drastically for dry atmosphere setups (factor 4 reduction to ( $\sim 0.12W/m^2$ )). Hence  
 765 this term is an important term in the TE budget. The TE budget for the dynamical core  
 766 is dominated by TE change due to hyperviscosity; TE errors due to time-truncation and  
 767 frictionless equations of motion are negligible. Errors associated with physics-dynamics  
 768 coupling (if applicable) are approximately  $0.5W/m^2$ . Due to the evolutionary nature of  
 769 model development the SE dynamical core’s continuous equation of motion conserve a  
 770 more comprehensive TE compared to the physical parameterizations. This TE discrep-  
 771 acy leads to an approximately  $0.5W/m^2$  total energy source. Running physics on a dif-  
 772 ferent grid than the dynamical introduces TE mapping errors such as in CAM-SE-CSLAM

773 (Conservative Semi-Lagrangian Multi-tracer transport scheme). These errors are, however,  
 774 rather small  $-0.07W/m^2$ .

775 A purpose of this paper is to better understand the energy characteristics of CAM  
 776 and to encourage modeling groups to perform similar analysis to better understand the  
 777 total energy flow in the atmospheric component of Earth system models. As has been  
 778 demonstrated in this paper there can easily be compensating errors in the system which  
 779 can not be identified without a detailed TE analysis.

### 780 Acknowledgments

781 The National Center for Atmospheric Research is sponsored by the National Science Foundation.  
 782 Computing resources (doi:10.5065/D6RX99HX) were provided by the Climate  
 783 Simulation Laboratory at NCAR's Computational and Information Systems Laboratory,  
 784 sponsored by the National Science Foundation and other agencies. The data used to per-  
 785 form the energy analysis can be found at <https://github.com/PeterHjortLauritzen/2018-JAMES-energy>.  
 786

### 787 References

- 788 Boville, B. (2000), chap. Toward a complete model of the climate system in Numerical  
 789 Modeling of the Global Atmosphere in the Climate System, pp. 419–442, Springer  
 790 Netherlands.
- 791 Computational and Information Systems Laboratory (2017), Cheyenne: HPE/SGI ICE XA  
 792 System (Climate Simulation Laboratory), Boulder, CO: National Center for Atmospheric  
 793 Research, doi:10.5065/D6RX99HX.
- 794 Eldred, C., and D. Randall (2017), Total energy and potential enstrophy conserv-  
 795 ing schemes for the shallow water equations using hamiltonian methods – part  
 796 1: Derivation and properties, *Geosci. Model Dev.*, 10(2), 791–810, doi:10.5194/  
 797 gmd-10-791-2017.
- 798 Gross, M., H. Wan, P. J. Rasch, P. M. Caldwell, D. L. Williamson, D. Klocke,  
 799 C. Jablonowski, D. R. Thatcher, N. Wood, M. Cullen, B. Beare, M. Willett, F. Lemarié,  
 800 E. Blayo, S. Malardel, P. Termonia, A. Gassmann, P. H. Lauritzen, H. Johansen, C. M.  
 801 Zarzycki, K. Sakaguchi, and R. Leung (2018), Physics-dynamics coupling in weather,  
 802 climate and earth system models: Challenges and recent progress, *Mon. Wea. Rev.*, 146,  
 803 3505–3544, doi:10.1175/MWR-D-17-0345.1.
- 804 Held, I. M., and M. J. Suarez (1994), A proposal for the intercomparison of the dynamical  
 805 cores of atmospheric general circulation models, *Bull. Amer. Meteor. Soc.*, 75, 1825–  
 806 1830.
- 807 Herrington, A. R., P. H. Lauritzen, M. A. Taylor, S. Goldhaber, B. E. Eaton, K. A. Reed,  
 808 and P. A. Ullrich (2018), Physics-dynamics coupling with element-based high-order  
 809 Galerkin methods: quasi equal-area physics grid, *Mon. Wea. Rev.*
- 810 Jablonowski, C., and D. L. Williamson (2011), chap. The Pros and Cons of Diffusion,  
 811 Filters and Fixers in Atmospheric General Circulation Models, pp. 381–493, Springer  
 812 Berlin Heidelberg, Berlin, Heidelberg, doi:10.1007/978-3-642-11640-7\_13.
- 813 Kasahara, A. (1974), Various vertical coordinate systems used for numerical weather pre-  
 814 diction, *Mon. Wea. Rev.*, 102(7), 509–522.
- 815 Lauritzen, P. H., R. D. Nair, and P. A. Ullrich (2010), A conservative semi-Lagrangian  
 816 multi-tracer transport scheme (CSLAM) on the cubed-sphere grid, *J. Comput. Phys.*,  
 817 229, 1401–1424, doi:10.1016/j.jcp.2009.10.036.
- 818 Lauritzen, P. H., J. T. Bacmeister, T. Dubos, S. Lebonnois, and M. A. Taylor (2014),  
 819 Held-Suarez simulations with the Community Atmosphere Model Spectral Element  
 820 (CAM-SE) dynamical core: A global axial angular momentum analysis using Eule-  
 821 rian and floating Lagrangian vertical coordinates, *J. Adv. Model. Earth Syst.*, 6, doi:  
 822 10.1002/2013MS000268.

- 823 Lauritzen, P. H., J. T. Bacmeister, P. F. Callaghan, and M. A. Taylor (2015), NCAR\_Topo  
 824 (v1.0): NCAR global model topography generation software for unstructured grids,  
 825 *Geosci. Model Dev.*, 8(12), 3975–3986, doi:10.5194/gmd-8-3975-2015.
- 826 Lauritzen, P. H., M. A. Taylor, J. Overfelt, P. A. Ullrich, R. D. Nair, S. Goldhaber, and  
 827 R. Kelly (2017), CAM-SE-CSLAM: Consistent coupling of a conservative semi-  
 828 lagrangian finite-volume method with spectral element dynamics, *Mon. Wea. Rev.*,  
 829 145(3), 833–855, doi:10.1175/MWR-D-16-0258.1.
- 830 Lauritzen, P. H., R. Nair, A. Herrington, P. Callaghan, S. Goldhaber, J. Dennis, J. T.  
 831 Bacmeister, B. Eaton, C. Zarzycki, M. A. Taylor, A. Gettelman, R. Neale, B. Dobbins,  
 832 K. Reed, and T. Dubos (2018), NCAR release of CAM-SE in CESM2.0: A reformu-  
 833 lation of the spectral-element dynamical core in dry-mass vertical coordinates with  
 834 comprehensive treatment of condensates and energy, *J. Adv. Model. Earth Syst.*, doi:  
 835 10.1029/2017MS001257.
- 836 Lin, S.-J. (2004), A 'vertically Lagrangian' finite-volume dynamical core for global mod-  
 837 els, *Mon. Wea. Rev.*, 132, 2293–2307.
- 838 McRae, A. T. T., and C. J. Cotter (2013), Energy- and enstrophy-conserving schemes for  
 839 the shallow-water equations, based on mimetic finite elements, *Quart. J. Roy. Meteor.  
 840 Soc.*, 140(684), 2223–2234, doi:10.1002/qj.2291.
- 841 Medeiros, B., D. L. Williamson, and J. G. Olson (2016), Reference aquaplanet climate in  
 842 the community atmosphere model, version 5, *J. Adv. Model. Earth Syst.*, 8(1), 406–424,  
 843 doi:10.1002/2015MS000593.
- 844 Neale, R. B., and B. J. Hoskins (2000), A standard test for AGCMs including their phys-  
 845 ical parametrizations: I: the proposal, *Atmos. Sci. Lett.*, 1(2), 101–107, doi:10.1006/asle.  
 846 2000.0022.
- 847 Neale, R. B., C.-C. Chen, A. Gettelman, P. H. Lauritzen, S. Park, D. L. Williamson, A. J.  
 848 Conley, R. Garcia, D. Kinnison, J.-F. Lamarque, D. Marsh, M. Mills, A. K. Smith,  
 849 S. Tilmes, F. Vitt, P. Cameron-Smith, W. D. Collins, M. J. Iacono, R. C. Easter, S. J.  
 850 Ghan, X. Liu, P. J. Rasch, and M. A. Taylor (2012), Description of the NCAR Commu-  
 851 nity Atmosphere Model (CAM 5.0), *NCAR Technical Note NCAR/TN-486+STR*, National  
 852 Center of Atmospheric Research.
- 853 Skamarock, W. C., J. B. Klemp, M. G. Duda, L. Fowler, S.-H. Park, and T. D. Ringler  
 854 (2012), A multi-scale nonhydrostatic atmospheric model using centroidal Voronoi tes-  
 855 selations and C-grid staggering, *Mon. Wea. Rev.*, 240, 3090–3105, doi:doi:10.1175/  
 856 MWR-D-11-00215.1.
- 857 Starr, V. P. (1945), A quasi-Lagrangian system of hydrodynamical equations., *J. Atmos.  
 858 Sci.*, 2, 227–237.
- 859 Taylor, M. A. (2011), Conservation of mass and energy for the moist atmospheric prim-  
 860 itive equations on unstructured grids, in: P.H. Lauritzen, R.D. Nair, C. Jablonowski,  
 861 M. Taylor (Eds.), Numerical techniques for global atmospheric models, *Lecture Notes  
 862 in Computational Science and Engineering*, Springer, 2010, *in press.*, 80, 357–380, doi:  
 863 10.1007/978-3-642-11640-7\_12.
- 864 Thuburn, J. (2008), Some conservation issues for the dynamical cores of NWP and cli-  
 865 mate models, *J. Comput. Phys.*, 227, 3715–3730.
- 866 Trenberth, K. E., and J. T. Fasullo (2018), Applications of an updated atmospheric ener-  
 867 getics formulation, *J. Climate*, 31(16), 6263–6279, doi:10.1175/JCLI-D-17-0838.1.
- 868 Wan, H., P. J. Rasch, M. A. Taylor, and C. Jablonowski (2015), Short-term time step con-  
 869 vergence in a climate model, *J. Adv. Model. Earth Syst.*, 7(1), 215–225, doi:10.1002/  
 870 2014MS000368.
- 871 Williamson, D. L. (2002), Time-split versus process-split coupling of parameterizations  
 872 and dynamical core, *Mon. Wea. Rev.*, 130, 2024–2041.
- 873 Williamson, D. L., and J. G. Olson (2003), Dependence of aqua-planet simulations on  
 874 time step, *Q. J. R. Meteorol. Soc.*, 129(591), 2049–2064.
- 875 Williamson, D. L., J. G. Olson, C. Hannay, T. Toniazzo, M. Taylor, and V. Yudin (2015),  
 876 Energy considerations in the community atmosphere model (cam), *J. Adv. Model. Earth*

- 877 *Syst.*, 7(3), 1178–1188, doi:10.1002/2015MS000448.  
878 Zhang, K., P. J. Rasch, M. A. Taylor, H. Wan, L.-Y. R. Leung, P.-L. Ma, J.-C. Golaz,  
879 J. Wolfe, W. Lin, B. Singh, S. Burrows, J.-H. Yoon, H. Wang, Y. Qian, Q. Tang,  
880 P. Caldwell, and S. Xie (2017), Impact of numerical choices on water conservation in  
881 the e3sm atmosphere model version 1 (eam v1), *Geoscientific Model Development Dis-*  
882 *cussions*, 2017, 1–26, doi:10.5194/gmd-2017-293.

```

do nt=1,ntotal

PARAMETERIZATIONS:
Last dynamics state received from dynamics
output 'pBF'
efix Energy fixer
output 'pBP'
phys param Physics updates the state and state saved for energy fixer
output 'pAP'
pwork Pressure work (dry mass correction)
output 'pAM'
Physics tendency (forcing) passed to dynamics

DYNAMICAL CORE
output 'dED'
do ns=1,nsplit
output 'dAF'

phys
START PHYSICS-DYNAMICS COUPLING
Update dynamics state with (1/nsplit) of physics tendency (ftype=2)
if (ns=1) Update dynamics state with entire physics tendency (ftype=1)
DONE PHYSICS-DYNAMICS COUPLING

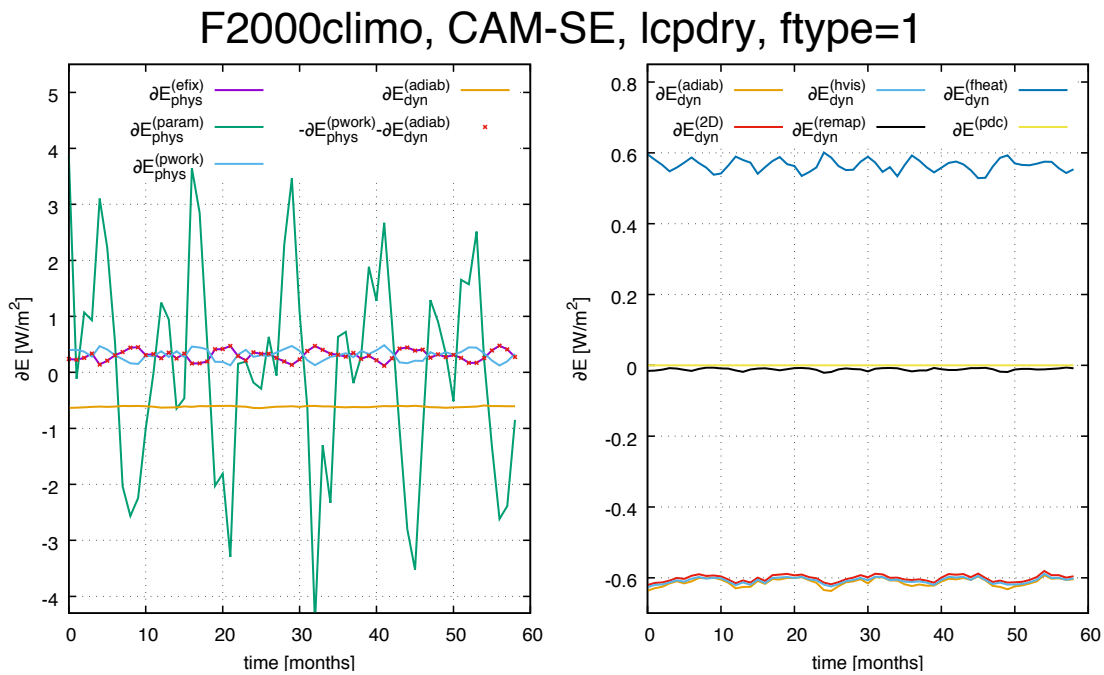
output 'dB'D'

adiab
2D
do nr=1,rsplit
Advance the adiabatic frictionless equations of motion
in floating Lagrangian layer
do ns=1,hypervis_subcycle
output 'dBH'
hvis
fheat Apply hyperviscosity operators
output 'dCH'
Add frictional heating to temperature
output 'dAH'
end do (ns=1,hypervis_subcycle)
end do (nr=1,rsplit)
output 'dAD'
remap
Vertical remapping from floating Lagrangian levels to Eulerian levels
output 'dAR'
end do (ns=1,nsplit)
Dynamics state saved for next model time step and passed to physics
output 'dB'F'

end do (nt=1,ntotal)

```

315 **Figure 1.** Pseudo-code for CAM-SE showing the order in which relevant physics updates are performed as  
 316 well as dynamical core steps and associated loops. In green font locations where the state is captured and out-  
 317 put is shown together with its 3 character identifier. The outer most loop (1, *ntotal*) advances the entire model  
 318  $\Delta t_{phys}$  seconds (in this case 1800s). The dynamical core loops are as follows: the outer loop is the vertical  
 319 remapping loop (1, *nsplit*) with associated time-step  $\Delta t_{phys}/nsplit$ . For stability the temporal advance-  
 320 ment of the equations of motion in the Lagrangian layer needs to be sub-cycled *rsplit* times. Within the  
 321 *rsplit*-loop the hyperviscosity time-stepping is sub-cycled *hypervis\_subcycle* times (again for stability).  
 322 For more details on the time-stepping in CAM-SE see Lauritzen *et al.* [2018].



464 **Figure 2.** Monthly averaged TE tendencies as a function of time for various aspects of the TE consistent  
 465 configuration of CAM-SE run in AMIP-type configuration with perpetual year 2000 SSTs. Left Figure shows  
 466  $\partial \hat{E}$  TE tendencies in physics and, for comparison, TE tendency for the adiabatic dynamical core. The right  
 467 plot shows the **breakdown** of  $\partial \hat{E}$  for the dynamical core. These plots show that the energy tendency from the  
 468 dynamical core is quite constant (to within  $\sim 0.02 W/m^2$  or less) so only one month simulations is adequate to  
 469 assess energy diagnostics for the dynamical core. For more details see Section 3.1.

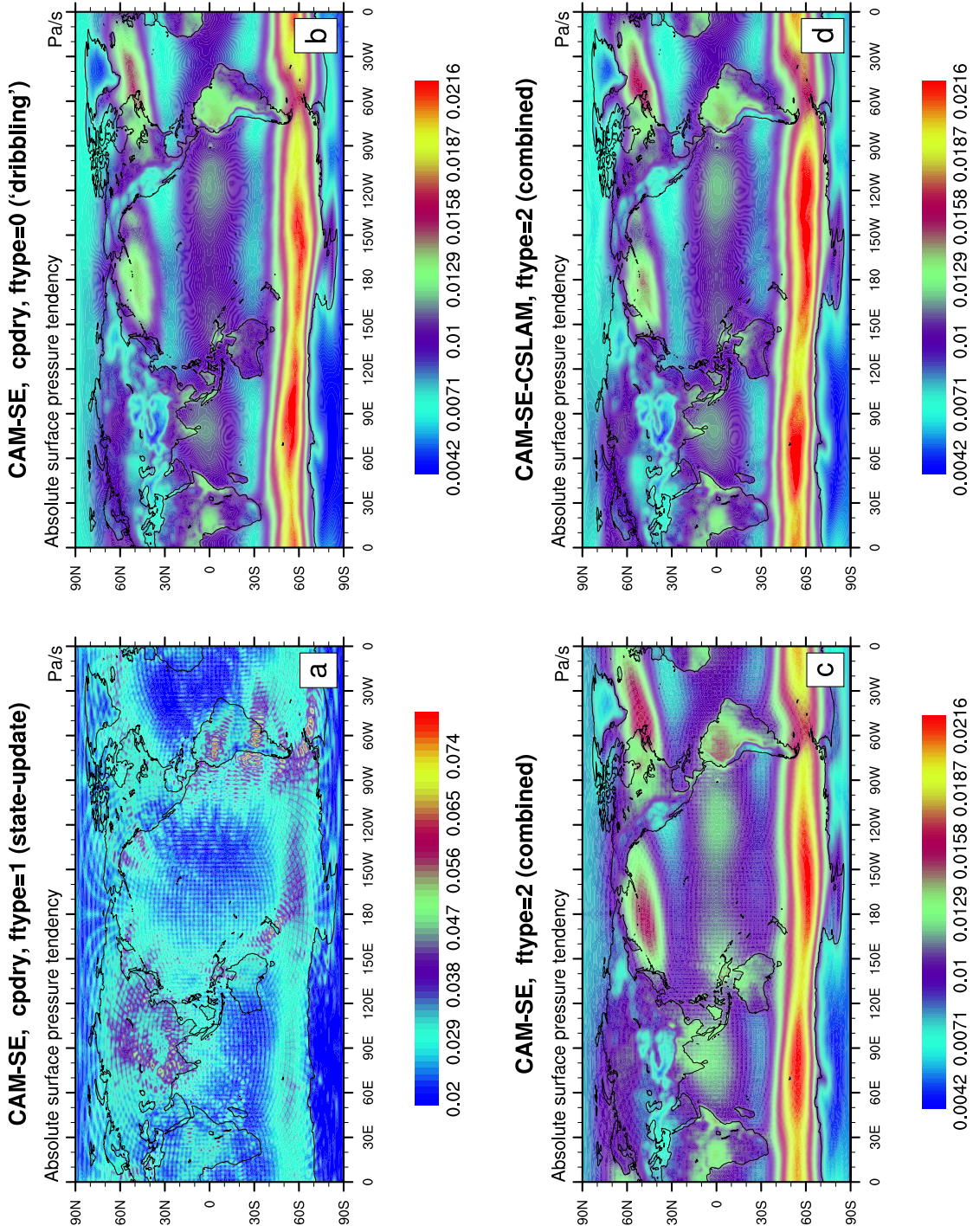


**Figure 3.** One year average of the absolute surface pressure tendency for (a) the TE consistent configuration, (b) ‘dribbling’ physics-dynamics coupling, (c) ftype=2 physics-dynamics coupling and (d) CSLAM version of CAM-SE, respectively. (a) has a closed physics-dynamics coupling budget but spurious noise, (b) has no spurious noise but the mass-budget in physics-dynamics coupling is not closed (see Figure 6), (c) has a closed mass budget in physics-dynamics coupling but some spurious noise at element boundaries which is eliminated when using CAM-SE-CSLAM (d). Note, the smallest value in panel (a) is the largest in panels (b), (c) and (d).

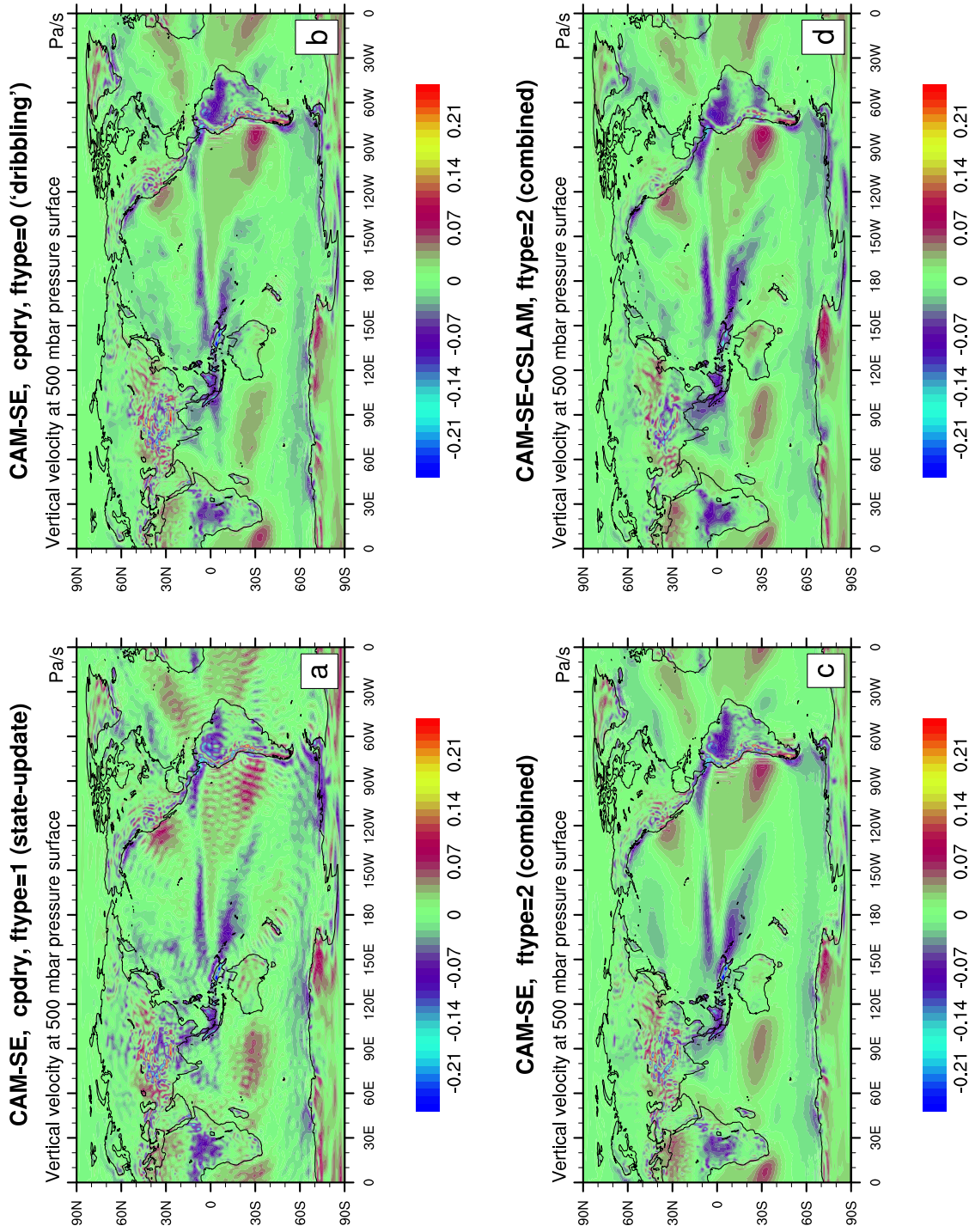


**Figure 4.** Same as Figure 3 but for 500hPa vertical pressure velocity. Note the ringing patterns off the West coast of South America and around the Himalayas in CAM-SE (a-c) that are eliminated with CAM-SE-CSLAM (d) that makes use of a quasi equal-area physics grid.

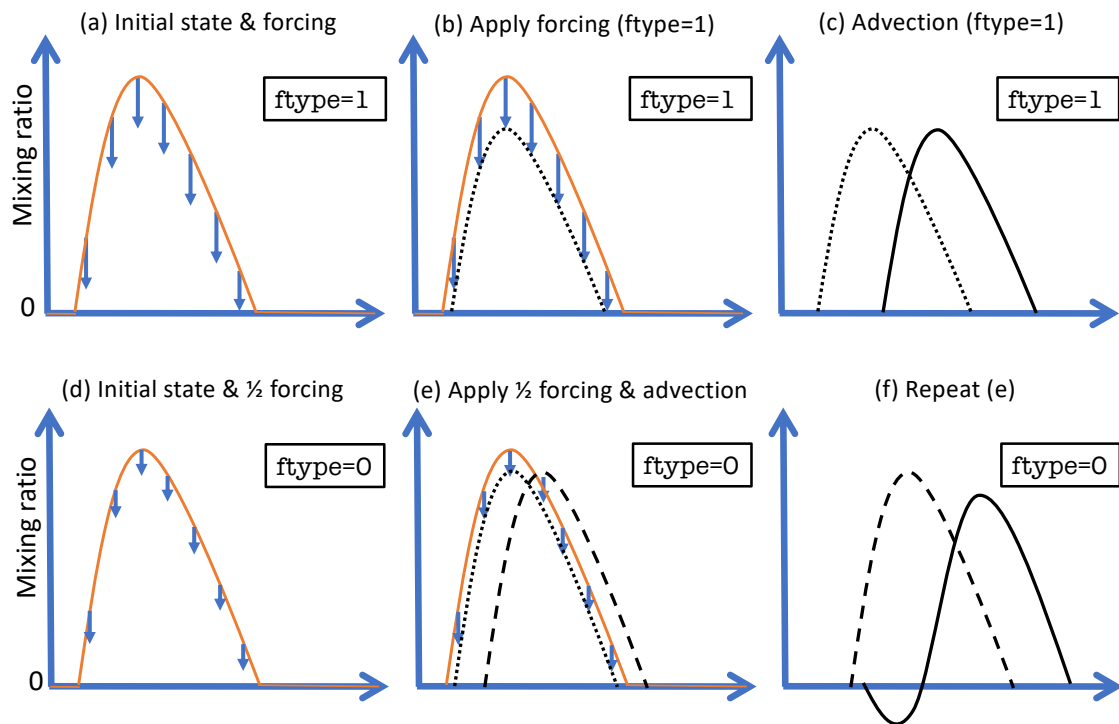


**Figure 5.** A schematic of state-update ( $\text{ftype}=1$ ; row 1) and ‘dribbling’ ( $\text{ftype}=0$ ; row 2) physics-dynamics coupling algorithms. See Section 3.2 for details.

## F2000climo, CAM-SE, cpdry, ftype=0 ('dribbling')

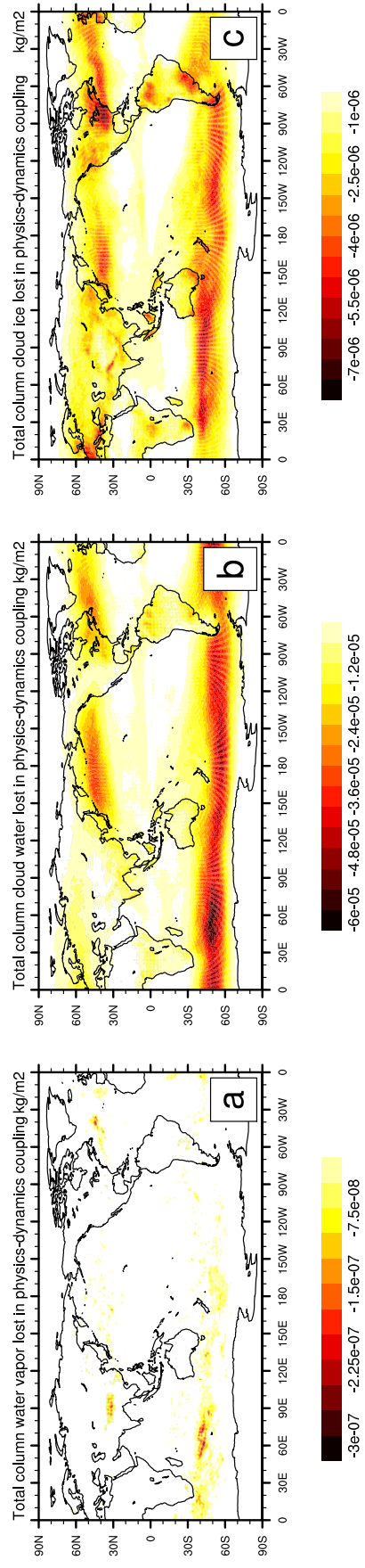


**Figure 6.** One year average of mass  $[kg/m^2]$  'clipped' in physics-dynamics coupling (so that state is not driven negative) when using `ftype=0` ('dribbling') physics-dynamics coupling for (a) water vapor, (b) cloud liquid and (c) cloud ice, respectively. Interestingly the element boundaries systematically show in the plots which is likely related to the anisotropy of the quadrature grid [Herrington *et al.*, 2018].

### TE tendencies for the default CAM-SE configuration (AMIP)

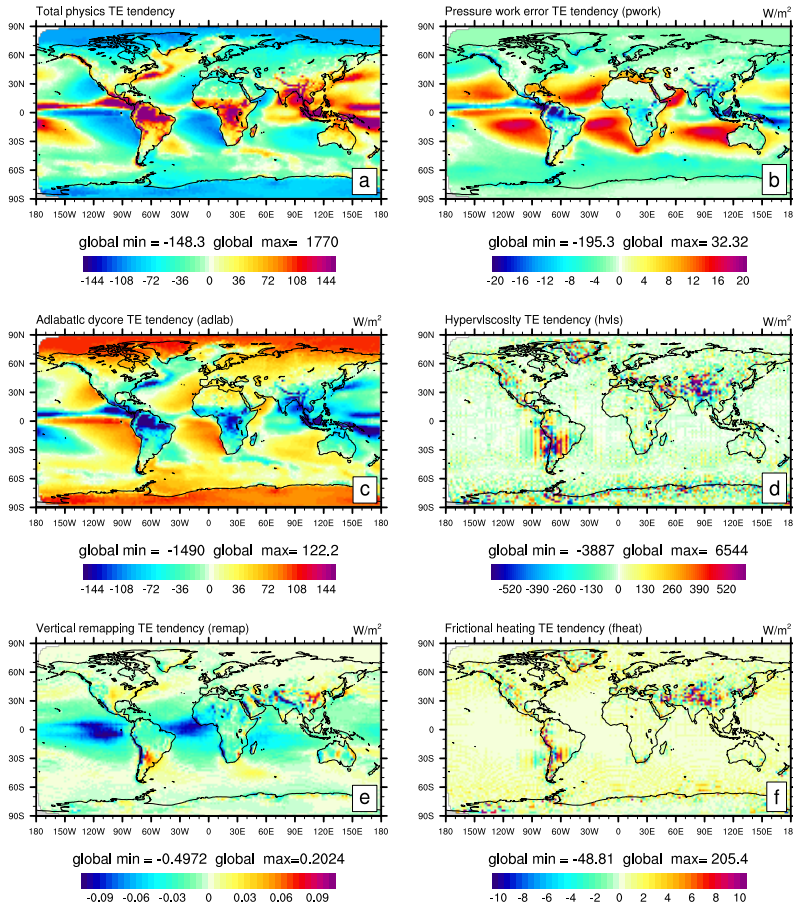


**Figure 7.** Two-dimensional spatial structure of column-integrated TE tendencies for different terms in the TE tendency budget using the *default* configuration: Column-integrated (a)  $\partial E^{(param)}$ ,  $\partial E^{(pwork)}$ ,  $\partial E^{(adiab)}$ ,  $\partial E^{(hvvis)}$ ,  $\partial E^{(remap)}$ , and  $\partial E^{(fheat)}$ . Above each color bar the global minimum and maximum TE tendencies are noted as there a small number of grid points where the TE tendencies are much larger than the color bar range.